Journal of Sound and Vibration (1998) **209**(1), 99–121

RESPONSE OF A MULTI-LAYERED INFINITE CYLINDER TO A PLANE WAVE EXCITATION BY MEANS OF TRANSFER MATRICES

J. S. Sastry

Aeroelasticity and Structural Dynamics Group, *Aeronautical Development Agency*, *Bangalore* 560 017, *India*

AND

M. L. Munjal

Centre of Excellence for Technical Acoustics, *Department of Mechanical Engineering*, *Indian Institute of Science*, *Bangalore*-560 012, *India*

(*Received* 14 *May* 1994, *and in final form* 4 *August* 1997)

A 4×4 transfer matrix is derived to evaluate the response of a multi-layered infinitely long elastic cylinder imbedded in a fluid and enclosing another fluid, to a given one-dimensional pressure excitation, or alternatively to evaluate the acoustic pressure distribution excited by the radial velocity component of the radiating surface. It is shown that the transfer matrix can be effectively used to obtain the scattering coefficient and noise reductiion of a multi-layered cylinder for the case of normal incidence of a plane wave. Expressions for several particular cases, such as monostatic back scattering, scattering from a rigid cylinder and a soft cylinder, a solid and a fluid cylinder, are presented. It is shown analytically that the expressions for scattering coefficient for the general case of a hollow cylinder and the particular cases of a fluid cylinder and a solid cylinder lead to the same expressions obtained by using a normal mode solution. Numerical results for the scattering form function and noise reduction of a two-layer infinite cylinder are given to illustrate the effect of layer material characteristics, variation of thickness of either of the constituent layers, cylinder dimensions, and ambient media. Finally, a four-layer hose has been analyzed in order to demonstrate the computational advantage of the transfer matrix method.

1. INTRODUCTION

Design of algorithms that estimate the target parameters by means of a cylindrical sonar system calls for the knowledge and understanding of response of the cylindrical shell housing the transducer array as well as scattering and transmission of incident acoustic wave. The incident acoustic wave could be an echo, radiated noise of the target, or that from the vehicle's own propeller that induces the self-noise to the system. Besides, the magnitude of turbulent wall pressure fluctuations that are transmitted through the cylindrical shell and sensed by the transducer inside has a significant bearing on the signal to noise ratio and demands precise estimation for the design of an efficient target detection system.

The studies concerning these phenomena for the case of cylinders have been made by contemporary researchers using the classical normal mode solutions, resonance scattering theory, the Sommerfeld–Watson transformation and a T-matrix approach. The classical

0022–460X/98/010099 + 23 $25.00/0/sv971262

normal mode solution of evaluating response of the cylindrical shell to a given pressure excitation and associated wave propagation involves expressing the displacements and stresses in terms of the scalar and vector potential functions and formulating the characteristic equations in terms of their amplitudes in individual layers by satisfying the interfacial and boundary conditions [1–5]. Resonance scattering adapted from nuclear scattering theory has been used to obtain the scattered field and response to surface waves by constructing the partial waves and obtaining the backgrounds and resonances from it [6, 7]. The Sommerfeld–Watson transformation has been applied to the normal mode series solution, and the resulting contour integrals are computed both by the saddle point method and by summing residues over poles which correspond to the zeros of a 6×6 determinant [8]. The T-matrix method consists of expanding the incident and scattered field quantities in appropriate vector basis functions depending upon the problem. The known incident field coefficients are related to unknown scattered field coefficients by means of a T-matrix [9, 10]. The classical normal mode technique has been used to obtain the scattered field due to a plane wave incident on a hollow cylinder [3] and a two-layered cylinder consisting of a visco-elastic coating on a metallic cylinder [5], in which 6×6 and 10×10 matrices have been formulated, respectively, to study acoustic scattering. The study of scattering from multiple concentric cylindrical shells with annular fluid layers [11] has been carried out essentially by using the 6×6 matrix developed for a single layer cylinder [7]. The scattered field due to oblique incidence [12], and the relation between resonances and surface waves in the scattering of oblique incident acoustic waves [13] have also been analyzed by using the same approach.

For the cases of a single-layered cylinder and a two-layered cylinder, the normal mode technique may seem to be appropriate. However, as the number of layers increases, the algebra associated with the formulation of characteristic equations become cumbersome (four characteristic equations for each additional layer) and the increase in the resultant matrix size (the matrix size being given by $(4n + 2) \times (4n + 2)$, where n is number of layers) makes computation of inverse or determinant of the coefficient matrix slower and some times may even lead to numerical difficulties. On the other hand, the transfer matrix approach which was originally proposed by Thomson [14] and followed by many others [15–17] is best suited for the analysis of multi-layer walls and passive acoustical filters [18], and is particularly suitable for digital computation.

In this paper, a 4×4 transfer matrix connecting the state variables on either side of the multi-layered infinitely long cylinder has been derived to obtain the response of the shell, and the scattering and transmission of a normally incident acoustic wave, in terms of elements of the overall transfer matrix. The model uses exact equations of elastodynamics, and construction of the solutions is made by using scalar and vector potentials. The solutions for the scalar and vector potentials in each layer are given in terms of Bessel functions. By using the interfacial conditions of continuity of pressure and radial velocity between the layers and appropriate radiation impedances on the exterior and interior of the multi-layered cylinder, explicit expressions for the response, scattering coefficient and transmission coefficient are obtained.

Expressions for the evaluation of wave propagation parameters such as the scattering coefficient and transmission coefficient in terms of elements of the transfer matrix have been obtained and these expressions can be directly used for any number of layers by noting that the elements of the final matrix are obtained after multiplication of the transfer matrices of the constituent layers. Thus, the resultant matrix would remain a 4×4 matrix irrespective of the number of layers.

Explicit expressions are given for the scattering form function and noise reduction in terms of matrix elements. Several interesting special cases such as monostatic back

scattering, scattering from a rigid cylinder and a soft cylinder, a solid cylinder and a fluid cylinder are discussed.

Analytical comparison of the scattering coefficient obtained by using the present transfer matrix is made with that obtained by using the normal mode solution [3] for the general case of a hollow cylinder and the particular cases of a fluid cylinder and a solid cylinder as the limiting cases. It is shown that both the methods lead to the same expressions if one uses equivalent notations (which necessitated evaluation of the determinants by using the matrix elements provided in the reference cited).

Expressions have also been derived to evaluate the response of the multi-layered cylinder to a given pressure excitation on one of the faces, with consideration taken of the boundary conditions of zero shear and appropriate radiation loading on the exposed faces. Similar expressions would hold for the acoustic pressure excited by the radial velocity component of the exposed surface.

Numerical examples are given for the case of a two layered cylinder consisting of a visco-elastic layer backed by a metallic cylinder. This configuration is chosen to increase understanding of the scattering behaviour of a multi-layer cylinder with damping material as the outer layer. Some parametric studies for different sizes of the visco-elastic layer and the metallic backing cylinder, with two different ambient fluids, have been carried out. In the limiting case of large radii, it is shown that the results for the multi-layered cylinder tend to those for a lined plate presented in reference [19].

2. BASIC EQUATIONS

The geometry considered for the present problem is shown in Figure 1. A plane wave is incident normal to the axis of symmetry of the multi-layered cylindrical shell, made up of m layers and having the inner and outer radii of each layer denoted by r'_{in} and r'_{out}, where i denotes the ith layer. The axis of the cylinder shell is taken to be the z-axis of the cylindrical co-ordinate system (r, θ, z). The cylinder is imbedded in a fluid having density ρ_0 and sound speed c_0 and encloses another fluid of density ρ_{m+1} and sound speed c_{m+1} inside of it. The topmost layer 1 and the bottommost layer m are in contact with the fluids. The four relevant state variables, normal stress σ_{rr}, shear stress $\tau_{r\theta}$, radial particle velocity V_r and the circumferential particle velocity V_θ at the two faces of the first layer are shown in Figure 2.

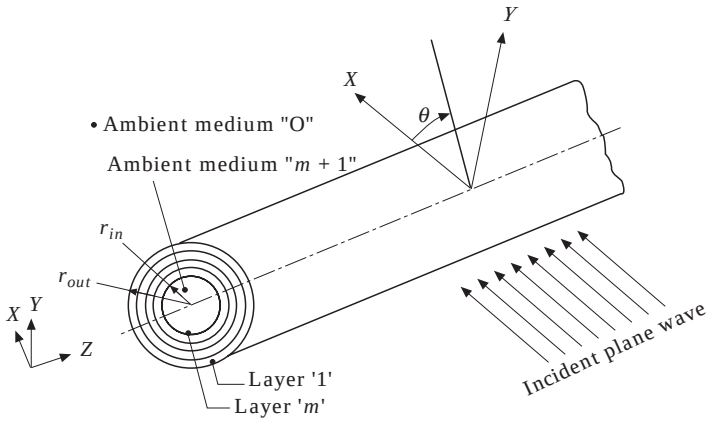

Figure 1. Geometry of multi-layered infinite cylinder with different wave components.

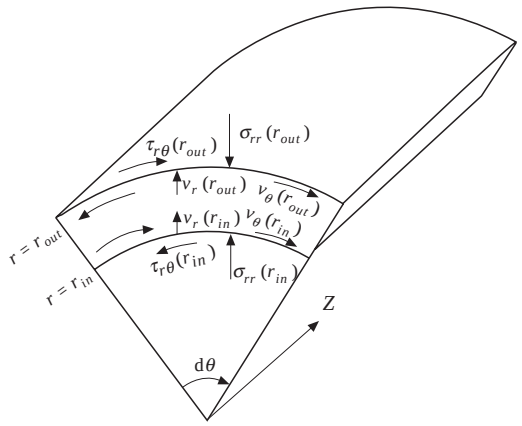

Figure 2. Co-ordinates and state variables at top and bottom faces of one layer of the multi-layered cylinder.

The two-dimensional components of the velocity vector $V(r, \theta)$ satisfying the field equation

$$\vec{V} = \text{grad } \phi + \text{curl } \vec{\varphi} \tag{1}$$

are given by

$$V_r = \partial\phi/\partial r + (1/r)\,\partial\varphi_z/\partial\theta, \qquad V_\theta = (1/r)\,\partial\phi/\partial\theta - \partial\varphi_z/\partial r, \tag{2, 3}$$

where ϕ is the scalar potential and $\vec{\varphi}$ is the vector potential. The radial stress σ_{rr} and shear stress $\tau_{r,\theta}$ are given by [20]

$$\sigma_{rr} = -\frac{2G}{j\omega}\left\{\frac{\partial V_r}{\partial r} + \frac{\mu}{1-2\mu}\left(\frac{V_r}{r} + \frac{1}{r}\frac{\partial V_\theta}{\partial\theta} + \frac{\partial V_r}{\partial r}\right)\right\}, \qquad \tau_{r\theta} = -\frac{G}{j\omega}\left(\frac{\partial V_\theta}{\partial r} - \frac{V_\theta}{r} + \frac{1}{r}\frac{\partial V_r}{\partial\theta}\right), \tag{4, 5}$$

where G denotes the shear modulus, μ the Poisson's ratio, and ω the circular frequency of excitation. Substituting equations (2) and (3) in equations (4) and (5) yields

$$\sigma_{rr} = -\frac{2G}{j\omega}\left\{\frac{\partial^2\phi}{\partial r^2} + \frac{1}{r}\frac{\partial^2\varphi_z}{\partial r\,\partial\theta} - \frac{1}{r^2}\frac{\partial\varphi_z}{\partial\theta} + \frac{\mu}{1-2\mu}\left(\frac{\partial^2\phi}{\partial r^2} + \frac{1}{r}\frac{\partial\phi}{\partial r} + \frac{1}{r^2}\frac{\partial^2\phi}{\partial\theta^2}\right)\right\}, \tag{6}$$

$$\tau_{r\theta} = -\frac{G}{j\omega}\left\{2\left(\frac{1}{r}\frac{\partial^2\phi}{\partial r\,\partial\theta} - \frac{1}{r^2}\frac{\partial\phi}{\partial\theta}\right) - \frac{\partial^2\varphi_z}{\partial r^2} + \frac{1}{r}\frac{\partial\varphi_z}{\partial r} + \frac{1}{r^2}\frac{\partial^2\varphi_z}{\partial\theta^2}\right\}. \tag{7}$$

By making use of the equations of motion [20]

$$G\{\text{div grad } \vec{V} + [1/(1-2\mu)]\,\text{grad div } \vec{V}\} = \rho\,\partial^2\vec{V}/\partial t^2, \tag{8}$$

it can be shown that ϕ and $\vec{\varphi}$ in equations (2), (3), (6) and (7) satisfy the wave equations [20]

$$G[2(1-\mu)/(1-2\mu)]\nabla^2_{r\theta}\phi = \rho\,\partial^2\phi/\partial t^2, \qquad G\nabla^2_{r\theta}\vec{\varphi} = \rho\,\partial^2\vec{\varphi}/\partial t^2, \tag{9, 10}$$

where $\nabla^2_{r\theta} = \partial^2/\partial r^2 + (1/r)\,\partial/\partial r + (1/r^2)\,\partial^2/\partial\theta^2$ is the Laplacian operator and ρ is the mass density. With the time dependence of all state variables being $\exp(j\omega t)$, the space dependence of ϕ and $\vec{\varphi}$ satisfy the Helmholtz equations

$$\nabla^2_{r\theta}\phi + k_L^2\phi = 0, \qquad \nabla^2_{r\theta}\vec{\varphi} + k_T^2\vec{\varphi} = 0, \tag{11, 12}$$

where

$$k_L^2 = \left(\frac{\omega}{c_L^2}\right)^2 = \frac{\omega^2\rho}{G}\frac{1-2\mu}{2(1-\mu)} = \frac{\omega^2\rho}{E}\frac{(1-2\mu)(1+\mu)}{(1-\mu)}, \qquad k_T^2 = \left(\frac{\omega}{c_T^2}\right)^2 = \frac{\omega^2\rho}{G}, \quad (13, 14)$$

and subscripts L and T denote longitudinal and transverse shear waves, respectively. c_L, the speed of longitudinal waves, and c_T, the speed of shear waves, are given by

$$c_L^2 = (G/\rho)2(1-\mu)/(1-2\mu), \qquad c_T^2 = G/\rho. \quad (15)$$

In the outside ambient fluid medium, the incident pressure and scattered pressure can be given by [2]

$$P_i(r, \theta, t) = \sum_{n=0}^{\infty} \varepsilon_n (-\mathrm{j})^n \mathrm{J}_n(k_0 r) \cos(n\theta)\, \mathrm{e}^{\mathrm{j}\omega t}, \quad (16)$$

$$P_s(r, \theta, t) = \sum_{n=0}^{\infty} \varepsilon_n (-\mathrm{j})^n b_n \mathrm{H}_n^{(2)}(k_0 r) \cos(n\theta)\, \mathrm{e}^{\mathrm{j}\omega t}. \quad (17)$$

As this paper is concerned with scattering coefficients normalized with respect to the incident wave, the amplitude of the incident wave in equation (16) has been taken to be unity.

The pressure field in the interior fluid of the multi-layered cylinder is given by

$$P_{m+1}(r, \theta, t) = \sum_{n=0}^{\infty} \varepsilon_n (-\mathrm{j})^n F_n \mathrm{J}_n(k_{m+1} r) \cos(n\theta)\, \mathrm{e}^{\mathrm{j}\omega t}. \quad (18)$$

General solutions of equations (9) and (10), for use in the layers of the cylinder, can be written as

$$\phi(r, \theta, t) = \sum_{n=0}^{\infty} \varepsilon_n (-\mathrm{j})^n \{A_n \mathrm{J}_n(k_L r) + B_n \mathrm{Y}_n(k_L r)\} \cos(n\theta)\, \mathrm{e}^{\mathrm{j}\omega t}, \quad (19)$$

$$\varphi_z(r, \theta, t) = \sum_{n=0}^{\infty} \varepsilon_n (-\mathrm{j})^n \{D_n \mathrm{J}_n(k_T r) + E_n \mathrm{Y}_n(k_T r)\} \sin(n\theta)\, \mathrm{e}^{\mathrm{j}\omega t}, \quad (20)$$

where $k_0 = \omega/c_0$, $k_{m+1} = \omega/c_{m+1}$, ω is the circular frequency, and c_0 and c_{m+1} are the speeds of sound in the exterior and interior ambient fluid media, respectively. $\varepsilon_n = 1$ for $n = 0$ and $\varepsilon_n = 2$ for $n \geqslant 1$. Here, $\mathrm{H}_n^{(2)} = \mathrm{J}_n - \mathrm{jY}_n$ are Hankel functions of the second kind, J_n and Y_n are Bessel and Neumann functions of order n, respectively. b_n, A_n, B_n, D_n, E_n and F_n are the scattering coefficients. Evaluation of the scattering coefficients b_n and F_n, and noise reduction constitute the present problem.

3. DERIVATION OF THE TRANSFER MATRIX

Substituting equations (19) and (20) in equations (2), (3), (6) and (7), one can obtain the state variables σ_{rr}, $\tau_{r\theta}$, V_r and V_θ for the first layer in terms of the constants A_n, B_n, D_n, E_n, and the inside and outside radii of the first layer.

Defining the identities,

$$\alpha_{n,1} \equiv A_n \, \mathrm{J}_n (k_L \, r) + B_n \, \mathrm{Y}_n (k_L \, r), \qquad \alpha_{n,2} \equiv A_n \, \mathrm{J}'_n (k_L \, r) + B_n \, \mathrm{Y}'_n (k_L \, r), \tag{21, 22}$$

$$\delta_{n,1} \equiv D_n \, \mathrm{J}_n (k_T \, r) + E_n \, \mathrm{Y}_n (k_T \, r), \qquad \delta_{n,2} \equiv D_n \, \mathrm{J}'_n (k_T \, r) + E_n \, \mathrm{Y}'_n (k_T \, r), \tag{23, 24}$$

one can write the state variables as

$$V_r = \sum_{n=0}^{\infty} \varepsilon_n (-\mathrm{j})^n \left(k_L \, \alpha_{n,2} + \frac{n}{r} \, \delta_{n,1} \right) \cos (n\theta), \tag{25}$$

$$V_\theta = \sum_{n=0}^{\infty} -\varepsilon_n (-\mathrm{j})^n \left(k_T \, \delta_{n,2} + \frac{n}{r} \, \alpha_{n,1} \right) \sin (n\theta), \tag{26}$$

$$\sigma_{rr} = \sum_{n=0}^{\infty} - \varepsilon_n (-\mathrm{j})^n \frac{2G}{\mathrm{j}\omega} \left[k_L^2 \left\{ \frac{n^2}{k_L^2 r^2} - \frac{(1-\mu)}{(1-2\mu)} \right\} \alpha_{n,1} - \frac{k_L}{r} \, \alpha_{n,2} - \frac{n}{r^2} \, \delta_{n,1} + \frac{n}{r} \, k_T \, \delta_{n,2} \right] \cos (n\theta), \tag{27}$$

$$\tau_{r\theta} = \sum_{n=0}^{\infty} - \varepsilon_n (-\mathrm{j})^n \frac{2G}{\mathrm{j}\omega} \left[\frac{n}{r^2} \, \alpha_{n,1} - \frac{n}{r} \, k_L \, \alpha_{n,2} + \frac{k_T}{r} \, \delta_{n,2} + \left\{ \frac{k_T^2}{2} - \frac{n^2}{r^2} \right\} \delta_{n,1} \right] \sin (n\theta). \tag{28}$$

The modal equations of the state variables can be written as

$$V_{r,n} = \left(k_L \, \alpha_{n,2} + \frac{n}{r} \, \delta_{n,1} \right), \qquad V_{\theta,n} = -\left(k_T \, \delta_{n,2} + \frac{n}{r} \, \alpha_{n,2} \right), \tag{29, 30}$$

$$\sigma_{rr,n} = -\frac{2G}{\mathrm{j}\omega} \left[k_L^2 \left\{ \frac{n^2}{k_L^2 r^2} - \frac{(1-\mu)}{(1-2\mu)} \right\} \alpha_{n,1} - \frac{k_L}{r} \, \alpha_{n,2} - \frac{n}{r^2} \, \delta_{n,1} + \frac{n}{r} \, k_T \, \delta_{n,2} \right], \tag{31}$$

$$\tau_{r\theta,n} = -\frac{2G}{\mathrm{j}\omega} \left[\frac{n}{r^2} \, \alpha_{n,1} - \frac{n}{r} \, k_L \, \alpha_{n,2} + \frac{k_T}{r} \, \delta_{n,2} + \left\{ \frac{k_T^2}{2} - \frac{n^2}{r^2} \right\} \delta_{n,1} \right]. \tag{32}$$

The modal equations of the state variables given above have been obtained by writing the state variables in terms of modal components as

$$V_r = \sum_{n=0}^{\infty} \varepsilon_n (-\mathrm{j})^n V_{r,n} \cos (n\theta), \qquad V_\theta = \sum_{n=0}^{\infty} \varepsilon_n (-\mathrm{j})^n V_{\theta,n} \sin (n\theta), \tag{33, 34}$$

$$\sigma_{rr} = \sum_{n=0}^{\infty} \varepsilon_n (-\mathrm{j})^n \sigma_{rr,n} \cos (n\theta), \qquad \tau_{r\theta} = \sum_{n=0}^{\infty} \varepsilon_n (-\mathrm{j})^n \sigma_{rr,n} \sin (n\theta). \tag{35, 36}$$

Solving equations (29–32) yields

$$\delta_{n,1} = (2/k_T^2) \{ -(\mathrm{j}\omega/2G) \tau_{r\theta,n} + V_{\theta,n} / r + (n/r) V_{r,n} \}, \tag{37}$$

$$\delta_{n,2} = (2/k_T^3) \{ -(\mathrm{j}\omega/2G) \, (n/r) \sigma_{rr,n} + (n^2/r^2 - k_T^2/2) V_{\theta,n} + (n/r^2) V_{r,n} \}, \tag{38}$$

$$\alpha_{n,1} = \{ (\mathrm{j}\omega/k_T^2 G) \sigma_{rr,n} - (2n^2/k_T^2 r^2) V_{\theta,n} \, r/n - 2V_{r,n}/k_T^2 r \}, \tag{39}$$

$$\alpha_{n,2} = \{ (\mathrm{j}\omega/k_T^2 G) \, (n/k_L \, r) \tau_{r\theta,n} - (2n/k_T^2 k_L \, r^2) V_{\theta,n} + (1 - 2n^2/k_T^2 r^2) V_{r,n}/k_L \}. \tag{40}$$

With use made of the recurrence relations of Bessel functions, the constants A_n, B_n, D_n and E_n can be obtained by solving simultaneously the system of equations (37–40).

At the exterior radius the state variables can be obtained from equations (29–32) and are given by

$$V_{r,n}(r_{out}) = \left[k_L \{A_n \, \mathrm{J}'_n (k_L \, r_{out}) + B_n \, \mathrm{Y}'_n (k_L \, r_{out})\} + \frac{n}{r_{out}} \{D_n \, \mathrm{J}_n (k_T \, r_{out}) + E_n \, \mathrm{Y}_n (k_T \, r_{out})\} \right], \quad (41)$$

$$V_{\theta,n}(r_{out}) = -\left[\frac{n}{r_{out}} \{A_n \, \mathrm{J}_n (k_L \, r_{out}) + B_n \, \mathrm{Y}_n (k_L \, r_{out})\} + K_T \{D_n \, \mathrm{J}'_n (k_T \, r_{out}) + E_n \mathrm{Y}'_n (k_T \, r_{out})\} \right], \quad (42)$$

$$\begin{aligned} \sigma_{rr,n} (r_{out}) = -\frac{2G}{\mathrm{j}\omega} \Bigg[& -\frac{k_T^2}{2} \left(1 - \frac{F}{r_{out}^2}\right) \{A_n \, \mathrm{J}_n (k_L \, r_{out}) + B_n \, \mathrm{Y}_n (k_L \, r_{out})\} \\ & - \frac{k_L}{r_{out}} \{A_n \, \mathrm{J}'_n (k_L \, r_{out}) + B_n \, \mathrm{Y}'_n (k_L \, r_{out})\} + \frac{k_T \, n}{r_{out}} \{D_n \, \mathrm{J}'_n (k_T \, r_{out}) + E_n \, \mathrm{Y}'_n (k_T \, r_{out})\} \\ & - \frac{n}{r_{out}^2} \{D_n \, \mathrm{J}_n (k_T \, r_{out}) + E_n \, \mathrm{Y}_n (k_T \, r_{out})\} \Bigg], \end{aligned} \quad (43)$$

$$\begin{aligned} \tau_{r\theta,n} (r_{out}) = -\frac{2G}{\mathrm{j}\omega} \Bigg[& \frac{n}{r_{out}^2} \{A_n \, \mathrm{J}_n (k_L \, r_{out}) + B_n \, \mathrm{Y}_n (k_L \, r_{out})\} - \frac{k_L \, n}{r_{out}} \{A_n \, \mathrm{J}_n (k_L \, r_{out}) \\ & + B_n \, \mathrm{Y}'_n (k_L \, r_{out})\} + \frac{k_T}{r_{out}} \{D_n \, \mathrm{J}'_n (k_T \, r_{out}) + E_n \, \mathrm{Y}'_n (k_T \, r_{out})\} \\ & + \frac{k_T^2}{2} \left(1 - \frac{F}{r_{out}^2}\right) \{D_n \, \mathrm{J}_n (k_T \, r_{out}) + E_n \, \mathrm{Y}_n (k_T \, r_{out})\} \Bigg], \end{aligned} \quad (44)$$

where

$$F = 2n^2/k_T^2. \quad (45)$$

Substitution of the constants A_n, B_n, D_n and E_n into equations (41–44) (the rather lengthy but straightforward algebraic details are omitted here), yields the following transfer matrix relationship between the state vector at (r_{out}, θ, n) and that at (r_{in}, θ, n):

$$\begin{bmatrix} \sigma_{rr,n} (r_{out}) \\ \tau_{r\theta,n} (r_{out}) \\ V_{\theta,n} (r_{out}) \\ V_{r,n} (r_{out}) \end{bmatrix} = \begin{bmatrix} A_{11} & A_{12} & A_{13} & A_{14} \\ A_{21} & A_{22} & A_{23} & A_{24} \\ A_{31} & A_{32} & A_{33} & A_{34} \\ A_{41} & A_{42} & A_{43} & A_{44} \end{bmatrix} \begin{bmatrix} \sigma_{rr,n} (r_{in}) \\ \tau_{r\theta,n} (r_{in}) \\ V_{\theta,n} (r_{in}) \\ V_{r,n} (r_{in}) \end{bmatrix}. \quad (46)$$

Elements A_{ij} of this transfer matrix are given in Appendix A.

4. EVALUATION OF SCATTERING AND TRANSMISSION COEFFICIENTS OF MULTI-LAYERED CYLINDER

Expressions for the transfer matrix elements given in Appendix A for the first layer can be used in evaluating the transfer matrices of the successive layers 2 to m as well. Then

the multi-layer system, comprising the exterior ambient medium "0", m successive layers and the interior medium $m+1$, can be represented by an overall transfer matrix, as given by

$$[S]_0 = [A]\,[S]_m, \tag{47}$$

where

$$[A] = [A]_1\,[A]_2 \ldots [A]_m. \tag{48}$$

$[A]$, the overall transfer matrix for the nth azimuthal mode, can be written as

$$\begin{bmatrix} \sigma_{rr,0,n} \\ \tau_{r\theta,0,n} \\ V_{\theta,0,n} \\ V_{r,0,n} \end{bmatrix} = \begin{bmatrix} A_{11} & A_{12} & A_{13} & A_{14} \\ A_{21} & A_{22} & A_{23} & A_{24} \\ A_{31} & A_{32} & A_{33} & A_{34} \\ A_{41} & A_{42} & A_{43} & A_{44} \end{bmatrix} \begin{bmatrix} \sigma_{rr,m,n} \\ \tau_{r\theta,m,n} \\ V_{\theta,m,n} \\ V_{r,m,n} \end{bmatrix}. \tag{49}$$

The ambient media in contact with layers 1 and m being fluids, shear stresses on both the exposed surfaces of the multi-layer system will be zero: i.e.,

$$\tau_{r\theta,0,n} = \tau_{r\theta,m,n} = 0. \tag{50}$$

The modal pressure and modal radial velocity on the exterior face are given by

$$P_{0,n} = \{\mathrm{J}_n\,(k_0\,r_{out}) + b_n\,\mathrm{H}_n^{(2)}(k_0\,r_{out})\}\cos(n\theta)\,\mathrm{e}^{\mathrm{j}\omega t}, \tag{51}$$

$$V_{r,0,n} = (\mathrm{j}/\rho_0\,c_0)\{\mathrm{J}_n'\,(k_0\,r_{out}) + b_n\,\mathrm{H}_n^{(2)'}(k_0\,r_{out})\}\cos(n\theta)\,\mathrm{e}^{\mathrm{j}\omega t}. \tag{52}$$

The modal impedances of the incident wave and scattered wave on the exterior surface are given by

$$Z_{0,n,i} = -\mathrm{j}\rho_0\,c_0\,(\mathrm{J}_n\,(k_0\,r_{out})/\mathrm{J}_n'\,(k_0\,r_{out}), \qquad Z_{0,n,s} = -\mathrm{j}\rho_0\,c_0\,(\mathrm{H}_n^{(2)}(k_0\,r_{out})/\mathrm{H}_n^{(2)'}(k_0\,r_{out}). \tag{53, 54}$$

The standing wave pressure is equal to normal compressive stress: i.e.,

$$\sigma_{rr,0,n} = P_{0,n}. \tag{55}$$

The corresponding relationships for the interior face are

$$P_{m,n} = F_n\,\mathrm{J}_n\,(k_{m+1}\,r_{in})\cos(n\theta), \qquad V_{r,m,n} = (\mathrm{j}F_n\,\mathrm{J}_n'\,(k_{m+1}\,r_{in})/\rho_{m+1}\,c_{m+1})\cos(n\theta), \tag{56, 57}$$

$$Z_{m+1,n} = -\mathrm{j}\rho_{m+1}\,c_{m+1}\,(\mathrm{J}_n\,(k_{m+1}\,r_{in})/\mathrm{J}_n'\,(k_{m+1}\,r_{in})), \qquad \sigma_{rr,m,n} = P_{m,n} = V_{r,m,n}\,Z_{m+1,n}, \tag{58, 59}$$

where $Z_{m+1,n}$ is the modal impedance exerted on the interior surface. The function $\cos(n\theta)\,\mathrm{e}^{\mathrm{j}\omega t}$ is common for modal pressure and modal radial velocity on both the exterior and interior faces, and therefore can be dropped henceforth for convenience of writing.

Substituting equations (50), (55) and (59) in the first of equations (49) yields

$$(A_{11}\,Z_{m+1,n} + A_{14})V_{r,m,n} + A_{13}\,V_{\theta,m,n} = P_{0,n}, \tag{60}$$

and substituting equations (50), (52) and (59) in the second of equations (49) yields

$$(A_{21}\,Z_{m+1,n} + A_{24})V_{r,m,n} + A_{23}\,V_{\theta,m,n} = 0. \tag{61}$$

Simultaneous solution of equations (60) and (61) yields

$$V_{r,m,n} = (P_{0,n}/DEN)A_{23}, \qquad V_{\theta,m,n} = -(A_{21}\,Z_{m+1,n} + A_{24})P_{0,n}/DEN, \tag{62, 63}$$

where

$$DEN = \{A_{23}\,(A_{11}\,Z_{m+1,n} + A_{14}) - A_{13}\,(A_{21}\,Z_{m+1,n} + A_{24})\}. \tag{64}$$

Substituting the values of $V_{r,m,n}$ and $V_{\theta,m,n}$ from equations (62) and (63) in the fourth of equations (49): i.e.,

$$V_{r,0,n} = A_{41}\,\sigma_{rr,m,n} = A_{43}\,V_{\theta,m,n} + A_{44}\,V_{r,m,n}, \tag{65}$$

one obtains

$$V_{r,0,n}\,\zeta = P_{0,n}, \tag{66}$$

where ζ represents the equivalent impedance of the complete passive sub-system consisting of layers 1 to m (whose impedance is denoted by ζ_L) and the radiation impedance exerted by the interior ambient fluid medium $m+1$ (whose impedance is denoted by Z_{m+1}).

The equivalent impedance $\zeta = f(\zeta_L, Z_{m+1})$ is given by

$$\zeta = \frac{\{A_{23}\,(A_{11}\,Z_{m+1,n} + A_{14}) - A_{13}\,(A_{21}\,Z_{m+1,n} + A_{24})\}}{\{A_{23}\,(A_{41}\,Z_{m+1,n} + A_{44}) - A_{43}\,(A_{21}\,Z_{m+1,n} + A_{24})\}} = \frac{M_1 + M_2\,/Z_{m+1}}{M_3 + M_4\,/Z_{m+1}}, \tag{67}$$

where

$$M_1 = (A_{11} - A_{13}\,A_{21}\,/A_{23}), \qquad M_2 = (A_{14} - A_{13}\,A_{24}\,/A_{23}), \tag{68a}$$

$$M_3 = (A_{11} - A_{43}\,A_{21}\,/A_{23}), \qquad M_4 = (A_{44} - A_{43}\,A_{24}\,/A_{23}). \tag{68b}$$

Substituting equations (51) and (52) into equation (66) yields an expression for the scattering coefficient b_n :

$$b_n = \{\rho_0\,c_0\,\mathrm{J_n}\,(k_0\,r_{out}) - \mathrm{j}\zeta\,\mathrm{J}'_n\,(k_0\,r_{out})\}/\{\mathrm{j}\zeta\,\mathrm{H}^{(2)'}_n(k_0\,r_{out}) - \rho_0\,c_0\,\mathrm{H}^{(2)}_n(k_0\,r_{out})\}. \tag{69}$$

It can readily be shown that equation (69) would be identical to the corresponding expression for the scattering coefficient in reference [3] if equivalent notation and co-ordinate transformation were used, and if the forms of equations (16) and (17) were the same as used in reference [3].

Upon making use of the expressions of modal incident and scattered wave impedances and surface impedances on the interior surface given in equations (53), (54) and (58), equation (69) turns out to be

$$b_n = [\mathrm{J}'_n\,(k_0\,r_{out})/\mathrm{H}^{(2)'}_n(k_0\,r_{out})]\Omega, \tag{70}$$

where

$$\Omega = -(\zeta - Z_{0,n,i})/(\zeta - Z_{0,n,s}). \tag{71}$$

Substitution of the expression of scattering coefficient given in equation (70) into equation (17) yields the expression for scattered pressure as

$$P_s = \sum_{n=0}^{\infty} \varepsilon_n\,(-\mathrm{j})^n\,\frac{\mathrm{J}'_n\,(k_0\,r_{out})}{\mathrm{H}^{(2)'}_n(k_0\,r_{out})}\,\Omega\mathrm{H}^{(2)}_n(k_0\,r_{out})\cos(n\theta). \tag{72}$$

In the far field, upon making use of the asymptotic representation for the Hankel function of second kind given in reference [21], one finds

$$\mathrm{H}^{(2)}_n = (2/\pi k_0\,r)^{0\cdot5}\exp\{-\mathrm{j}(k_0\,r - n\pi/2 - \pi/4)\}. \tag{73}$$

The far field scattered pressure in equation (72) is given by

$$P_s = \left(\frac{2\mathrm{j}}{\pi k_0 r_{out}}\right)^{0\cdot5} \exp(-\mathrm{j}k_0 r_{out}) \sum_{n=0}^{\infty} \varepsilon_n b_n \cos(n\theta). \tag{74}$$

Now, the scattering form function is defined as [12]

$$|f_\infty| = \frac{2}{(\pi k_0 r_{out})^{0\cdot5}} \left| \sum_{n=0}^{\infty} \varepsilon_n b_n \cos(n\theta) \right|. \tag{75}$$

For the case of monostatic back scattering, $\theta = \pi$, making $\cos(n\pi) = (-1)^n$, the expression for the scattering form function becomes

$$|f_\infty| = \frac{2}{(\pi k_0 r_{out})^{0\cdot5}} \left| \sum_{n=0}^{\infty} \varepsilon_n b_n (-1)^n \right|. \tag{76}$$

Substituting the expression for the scattering coefficient b_n in equation (51), and making use of equations (56–59), one obtains

$$F_n = \{\mathrm{J}_n(k_0 r_{out}) + b_n \mathrm{H}_n^{(2)}(k_0 r_{out})\} \frac{A_{23} Z_{m+1}}{DEN \mathrm{J}_n(k_{m+1} r_{in})}. \tag{77}$$

Substitution of this expression into equation (18) yields the pressure field transmitted through the shell:

$$P_{m+1} = \sum_{n=0}^{\infty} \varepsilon_n (-\mathrm{j})^n \{\mathrm{J}_n(k_0 r_{out}) + b_n \mathrm{H}_n^{(2)}(k_0 r_{out})\} \frac{A_{23} Z_{m+1,n}}{DEN} \cos(n\theta). \tag{78}$$

The noise reduction achieved by the cylindrical shell is given by

$$NR = 20 \log_{10} \left| \frac{(P_i + P_s)}{P_{m+1}} \right| = 20 \log_{10}$$

$$\times \left[\left| \frac{\displaystyle\sum_{n=0}^{\infty} \varepsilon_n (-\mathrm{j})^n \{\mathrm{J}_n(k_0 r_{out}) + b_n \mathrm{H}_n^{(2)}(k_0 r_{out})\} \cos(n\theta)}{\displaystyle\sum_{n=0}^{\infty} \varepsilon_n (-\mathrm{j})^n F_n \mathrm{J}_n(k_{m+1} r_{in}) \cos(n\theta)} \right| \right]. \tag{79}$$

For the case of monostatic back scattering, $\theta = \pi$, making $\cos(n\pi) = (-1)^n$, the expression for noise reduction becomes

$$NR = 20 \log_{10} \left| \frac{(P_i + P_s)}{P_{m+1}} \right| = 20 \log_{10}$$

$$\left[\left| \frac{\displaystyle\sum_{n=0}^{\infty} \varepsilon_n (-\mathrm{j})^n \{\mathrm{J}_n(k_0 r_{out}) + b_n \mathrm{H}_n^{(2)}(k_0 r_{out})\} (-1)^n}{\displaystyle\sum_{n=0}^{\infty} \varepsilon_n (-\mathrm{j})^n F_n \mathrm{J}_n(k_{m+1} r_{in}) (-1)^n} \right| \right]. \tag{80}$$

Some of the interesting particular cases of scattering can be drawn from the expression for the scattering coefficient given in equation (70).

In the expression for Ω, if the equivalent impedance characterized by ζ is very high compared to that of the modal impedance of the incident and scattered waves $Z_{0,n,i}$ and $Z_{0,n,s}$ ($\zeta \gg Z_{0,n,i}$ and $Z_{0,n,s}$), the scattering function would correspond to a rigid cylinder whose scattering coefficient is given by

$$b_n = -\mathrm{J}'_n(k_0 r_{out})/\mathrm{H}^{(2)'}_n(k_0 r_{out}). \tag{81}$$

On the other hand, if $\zeta \ll Z_{0,n,i}$ and $Z_{0,n,s}$, then the scattering function relates to a soft cylinder whose scattering coefficient is given by

$$b_n = -\mathrm{J}_n(k_0 r_{out})/\mathrm{H}^{(2)}_n(k_0 r_{out}). \tag{82}$$

The case of scattering by a fluid cylinder can be obtained if one lets $r_{in} \to r_{out}$, in the elements A_{ij} of the transfer matrix equation (49), which implies the absence of the multi-layer filter, and incidence of the wave on the interface of the exterior and interior fluids. In this case, as expected, the transfer matrix reduces to a unit matrix:

$$\begin{bmatrix} \sigma_{rr,0,n} \\ \tau_{r\theta,0,n} \\ V_{\theta,0,n} \\ V_{r,0,n} \end{bmatrix} = \begin{bmatrix} 1 & 0 & 0 & 0 \\ 0 & 1 & 0 & 0 \\ 0 & 0 & 1 & 0 \\ 0 & 0 & 0 & 1 \end{bmatrix} \begin{bmatrix} \sigma_{rr,m,n} \\ \tau_{r\theta,m,n} \\ V_{\theta,m,n} \\ V_{r,m,n} \end{bmatrix}. \tag{83}$$

Substitution of elements A_{ij} of this matrix into equation (67) yields the equivalent impedance as

$$\zeta = Z_{m+1}, \tag{84}$$

which confirms the absence of contribution of the impedance of the multi-layers to the equivalent impedance. Substitution of equation (84) into equation (69) yields an expression for the scattering coefficient for the case of a fluid cylinder:

$$b_n = \{\rho_0 c_0 \mathrm{J}_n(k_0 r_{out}) - \mathrm{j}Z_{m+1} \mathrm{J}'_n(k_0 r_{out})\}/\{\mathrm{j}Z_{m+1} \mathrm{H}^{(2)'}_n(k_0 r_{out}) - \rho_0 c_0 \mathrm{H}^{(2)}_n(k_0 r_{out})\}. \tag{85}$$

Equation (85) has been found to be identical to equation (13a) of reference [3], which in fact necessitated evaluation of the determinant with the elements presented in the reference cited, after the forms of equations (16) and (17) were changed to those of reference [3]. It may be noted that the denominator in equation (85) contains Hankel functions of the second kind, and derivatives thereof, as the outgoing waves are represented by $\mathrm{H}^{(2)}_n(k_0 r)$, to be consistent with the time dependence $\exp(\mathrm{j}\omega t)$ adopted in this paper.

The case of scattering from a solid cylinder can also be obtained from the transfer matrix equation (49). In this case, the elastic medium includes the origin, necessitating the condition of $B_n = D_n = F_n = 0$, to cater for the absence of Neumann functions. With this condition, and applying the limits [21]

$$\lim_{z \to 0} \mathrm{J}_n(z) \cong (z/2)^n/\Gamma(n+1), \qquad \lim_{z \to 0} \mathrm{Y}_0(z) \cong (2/\pi)\ln(z), \tag{86a, b}$$

$$\lim_{z \to 0} \mathrm{Y}_n(z) \cong (1/\pi)\Gamma(n)(z/2)^{-n}, \tag{86c}$$

each of the matrix elements of equation (46) (see Appendix A) now contain only the terms having the Bessel functions of the first kind and its derivatives. Substitution of the elements A_{ij} of this reduced matrix into the equation for equivalent impedance and scattering coefficient given by equations (67) and (69), respectively, and noting the absence of

radiation impedance exerted by the interior fluid Z_{m+1}, yields the following expressions for the equivalent impedance and scattering coefficient:

$$\zeta = \frac{\{A_{23}\, A_{14} - A_{13}\, A_{24}\}}{\{A_{23}\, A_{44} - A_{43}\, A_{24}\}}, \qquad b_n = \frac{\{\rho_0\, c_0\, \mathrm{J}_n\,(k_0\, r_{out}) - \mathrm{j}\zeta \mathrm{J}'_n\,(k_0\, r_{out})\}}{\{\mathrm{j}\zeta \mathrm{J}'_n\,(k_0\, r_{out}) - \rho_0\, c_0\, \mathrm{J}_n\,(k_0\, r_{out})\}}. \tag{87, 88}$$

The elements A_{ij} required to calculate the scattering coefficient for the particular case of solid cylinder are given in Appendix B.

Equation (88) has been verified to be identical to equations (12a, b) of reference [3], which again necessitated evaluation of the determinant with the elements presented in the reference cited.

5. RESPONSE OF THE MULTI-LAYERED CYLINDER TO EXTERNAL EXCITATION

The transfer matrix relation (49) can be used to evaluate the radial velocities at the two exposed surfaces of the multi-layer cylinder excited by an incident plane wave, or alternatively to evalute the acoustic pressure distribution excited by the radial velocity components of the radiating surfaces.

Let the modal external excitation on the exterior of the first layer have the distribution

$$P_{0,n} = \{\mathrm{J}_n\,(k_0\, r_{out}) + b_n\, \mathrm{H}_n^{(2)}(k_0\, r_{out})\} \cos\,(n\theta). \tag{89}$$

The resulting compressive stresses at the exposed surfaces $r = r_{in}$ and $r = r_{out}$ are given by

$$\sigma_{rr,n,0} = P_{0,n} - Z_{0,n}\, V_{r,0,n}, \qquad \sigma_{rr,n,m} = Z_{m+1,n}\, V_{r,m,n}, \tag{90, 91}$$

where $Z_{0,n}$ and $Z_{m+1,n}$ are the modal radiation impedances exerted by the ambient medium in contact when the first layer and mth layer, respectively (see equations (53), (54) and (58)). If the ambient media are fluids, they would not support any shear stresses. Then

$$\tau_{r\theta,0,n} = \tau_{r\theta,m,n} = 0. \tag{92}$$

By substituting the four boundary conditions (90–92) in the four equations of the transfer matrix equation (49), one can derive expressions for the radial velocities at the two exposed surfaces as follows. Making use of equations (90–92) and the first and fourth of equations (49) yields

$$P_{0,n} - Z_{0,n}\, V_{r,0,n} = (A_{11}\, Z_{m+1,n} + A_{14}) V_{r,m,n} + A_{13}\, V_{\theta,m,n}, \tag{93}$$

$$V_{r,0,n} = (A_{41}\, Z_{m+1,n} + A_{44}) V_{r,m,n} + A_{43}\, V_{\theta,m,n}. \tag{94}$$

Substituting equation (94) in equation (93) yields

$$V_{\theta,m,n} = [P_{0,n} - V_{r,m,n}\,(Z_{0,n}\, M_{41} + M_{11})]/(A_{13} + Z_{0,n}\, A_{43}). \tag{95}$$

Substituting equation (95) into the second of equations (49), and simplifying, one obtains

$$V_{r,m,n} = (A_{23}\,/DEN) P_{0,n}, \tag{96}$$

where

$$DEN = \{ -(A_{13}\, Z_{0,n} + A_{43}) M_{21} + (M_{41}\, Z_{0,n} + M_{11}) A_{23}\}, \tag{97}$$

$$M_{11} = A_{11}\, Z_{m+1,n} + A_{14}, \qquad M_{21} = A_{21}\, Z_{m+1,n} + A_{24}, \qquad M_{41} = A_{41}\, Z_{m+1,n} + A_{44}. \tag{98a–c}$$

Simultaneous solution of equations (93) and (94), and simplification, yields

$$V_{r,0,n} = \{A_{43} - A_{23}\,(A_{43}\, M_{11} - A_{13}\, M_{41})/DEN\} P_{0,n}\,/(A_{13} + Z_{0,n}\, A_{43}). \tag{99}$$

TABLE 1

Material constants

Material	Density (ρ)	Modulus of elasticity (E)	Poisson's ratio (μ)
Elastomer layer	1200	$3{\cdot}3 \times 10^8(1 + j0{\cdot}8)$	0·49
Backing steel layer	7800	$2{\cdot}1 \times 10^{11}(1 + j0{\cdot}002)$	0·31

TABLE 2

Ambient media constants

Ambient medium	Density (ρ)	Speed of sound (c_0)
Sea water	1025	1500
Air	1·18	340

6. NUMERICAL RESULTS

In order to illustrate the use of the transfer matrix developed to evaluate the scattering coefficient and noise reduction of a multi-layer infinite cylinder, for the case of normal incidence and one-dimensional pressure excitation, several numerical examples are presented. Unless otherwise specified, the configuration chosen is a two-layer infinite cylinder consisting of a carbon steel inner cylinder of 5 mm thickness lined with an outer elastomer cylindrical layer of 5 mm thickness. All the results are shown for the frequency range that is typical of the underwater acoustic applications for which the present model is primarily expected to be used. Default values of the outer and inner radius of the multi-layer cylinder are $r_{out} = 100$ mm and $r_{in} = 90$ mm ($r_{out} = 100$ mm and $r_{in} = 95$ mm for the elastomer cylinder, and $r_{out} = 95$ mm and $r_{in} = 90$ mm for the steel cylinder). Water and air are considered as the ambient medium outside and inside of the two-layer cylinder, respectively. The x-co-ordinate krsh $\equiv k_0 r_{out}$ in all the figures.

Values of density (in kg/m^3), Poisson's ratio and elastic modulus (in Pa) for the two constituent layers are given in Table 1. The presence of structural damping represented by a loss factor would make E and G and thence c_L and c_T, or k_L and k_T, complex, which

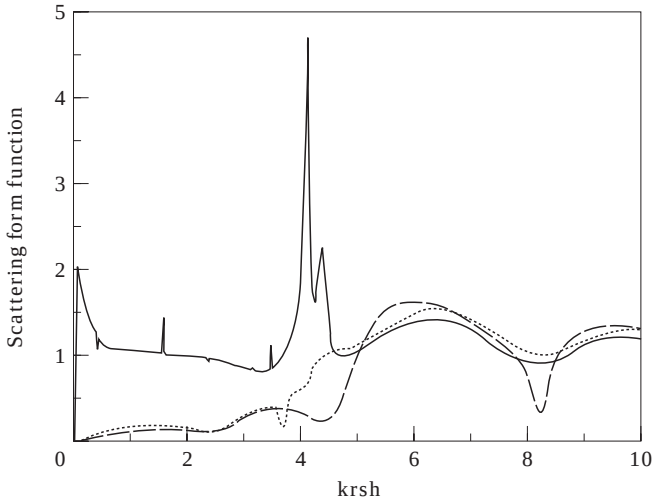

Figure 3. Effect of the cylinder wall composition on the scattering form function. ——, Elastomer; — —, steel; · · · ·, composite.

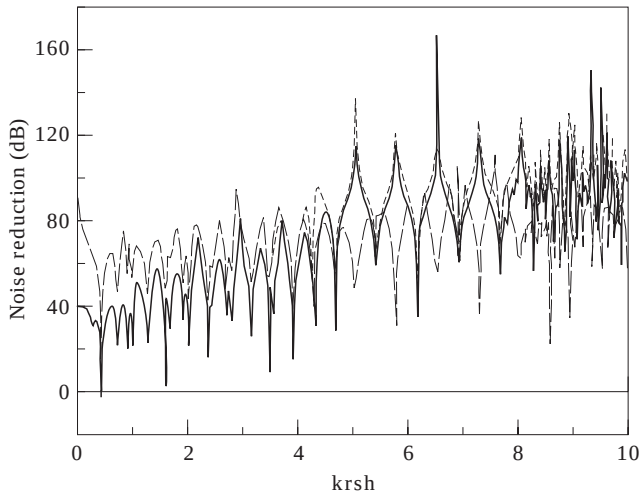

Figure 4. Effect of the cylinder wall composition on noise reduction. ——, Elastomer, — —, steel; - - - -, composite.

would make the arguments of the Bessel functions of all three kinds complex. The series representations for Bessel functions [21] are used in the computations.

Values of density and speed of sound (in m/s) for sea water and air (which are ambient media) are given in Table 2.

Figures 3 and 4 show the scattering form function and noise reduction for various layer configurations, respectively. Results are plotted for the cases of elastomer cylinder ($r_{out} = 100$ mm and $r_{in} = 95$ mm), backing steel cylinder ($r_{out} = 100$ mm and $r_{in} = 95$ mm), and combination of the two (lined cylinder, $r_{out} = 100$ mm and $r_{in} = 90$ mm). It can be observed from Figure 3, that there exist three regions of the scattering form function $|f_\infty|$. Region I comprises high and low values of $|f_\infty|$ for the elastomer cylinder and steel cylinder cases, respectively, up to a frequency of 10 kHz (krsh $\equiv k_0 r_{out} = 4{\cdot}0$). Region II is

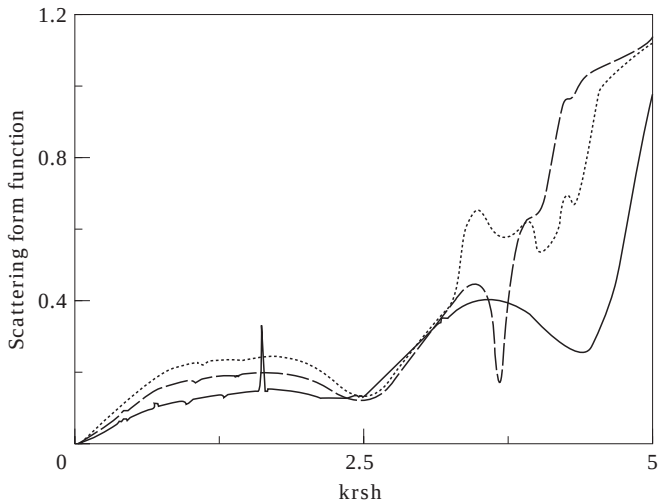

Figure 5. Effect of the elastomer lining thickness on the scattering form function. ——, Unlined; — —, th = 5 mm; · · · ·, th = 10 mm.

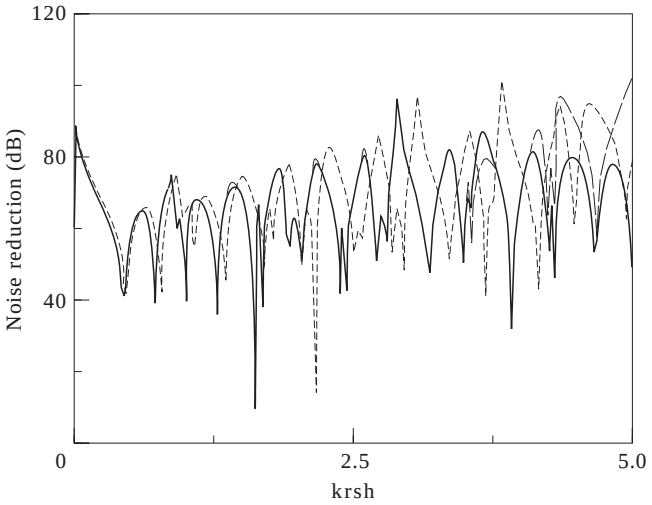

Figure 6. Effect of the elastomer lining thickness on noise reduction. ——, Unlined; — —, th = 5 mm, - - - -, th = 10 mm.

characteristic of structural resonances of metal or elastomer. There is a relative rise and fall in $|f_\infty|$, for elastomer cylinder and steel cylinder, respectively. Beyond 45 kHz ($k_0 r_{out} > 18{\cdot}0$), not shown here, there is a rapid fall in $|f_\infty|$ for all the three cases, and this region can be identified as Region III. As can be seen from Figure 4, there is an increase in the noise reduction for all the three cases. For the remaining curves, the non-dimensional frequency parameter krsh $\equiv k_0 r_{out}$ has been restricted to 5·0 (corresponding to about 12 000 Hz).

The effect of varying the thickness of elastomer layer on the scattering form function and noise reduction is shown in Figures 5 and 6, respectively, wherein the elastomer layer thickness is varied from 0 mm (which means backing steel cylinder alone) to 10 mm. The presence and variation of thickness of elastomer layer shifted the high amplitude

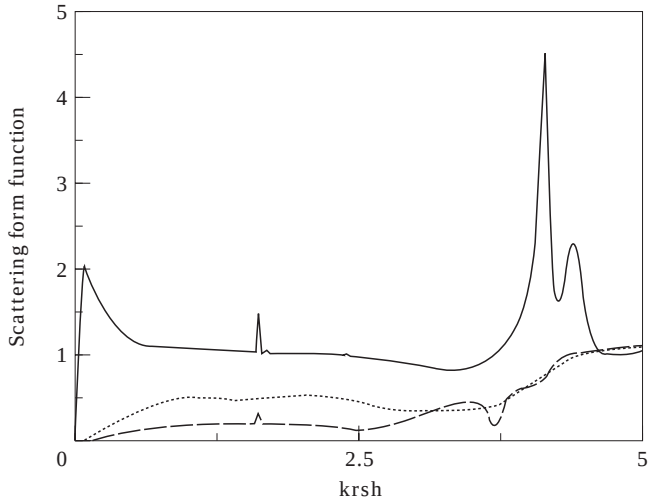

Figure 7. Effect of the steel backing layer thickness on the scattering form function. ——, No backing; — —, th = 5 mm; · · · ·, th = 10 mm.

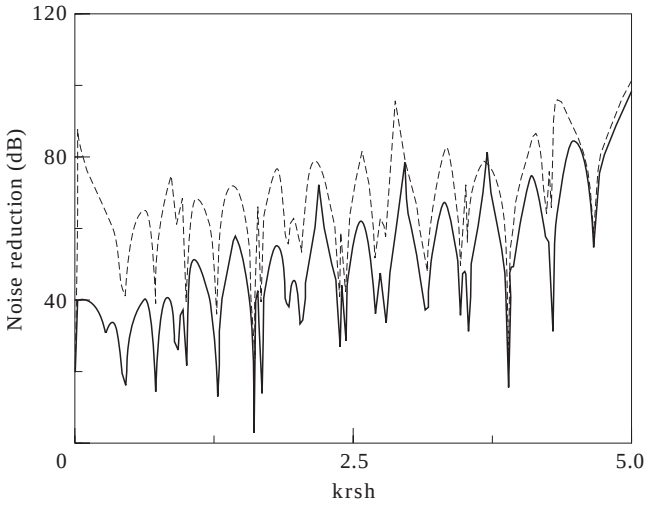

Figure 8. Effect of the steel backing layer thickness on noise reduction. ——, No backing; – – –, th = 5 mm.

resonances to relatively higher frequencies for both the scattering form function and noise reduction accompanied with slight changes in their values as the thickness is progressively varied.

The effect of varying the thickness of the backing steel cylinder on the scattering form function and noise reduction is presented in Figures 7 and 8. With increase in the thickness of the steel cylinder, more or less the same phenomenon as that of the increase in the elastomer layer is observed for the high amplitude peak, except for the magnitude.

The effect of the ambient media on the scattering form function and noise reduction is presented in Figures 9 and 10, respectively. While it is always water on the incidence side or outer side, it could be either air or water on the transmission side or inside. While the high frequency scattering behaviour is more or less the same for both the cases; the scattering form function is less in the water–water closure configuration at lower

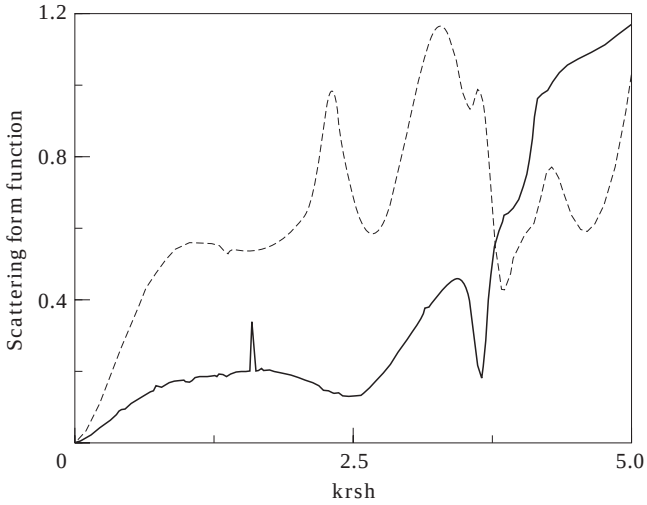

Figure 9. Effect of the ambient media on the scattering form function. ——, Water–air; – – –, water–water.

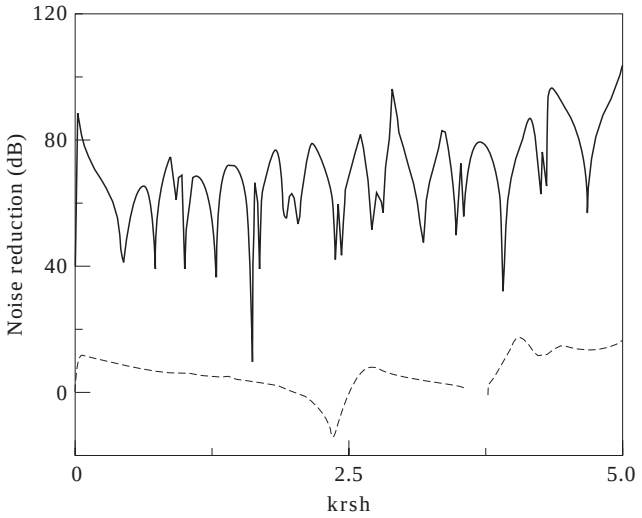

Figure 10. Effect of the ambient media on noise reduction. ——, Water–air; – – –, water–water.

frequencies. For the water–water case, the impedance mismatch is much weaker and this leads to very low values of noise reduction.

The effect of varying the size of the cylinder, keeping the same thickness, on the scattering form function and noise reduction is presented for two different sizes of metallic cylinder for krsh = 0–5 in Figures 11 and 12, and for a frequency range of 0–6000 Hz in Figures 13 and 14. In these figures, comparison is made between a smaller cylinder ($r_{out} = 100$ mm) and a larger cylinder ($r_{out} = 250$ mm). With increase in the radius, there is a shift of structural resonances towards lower frequencies as can be observed from Figure 14. This does not appear in the corresponding Figure 12 where the outer radius r_{out} is included in the non-dimensional frequency parameter or Helmholtz number in the abcissa.

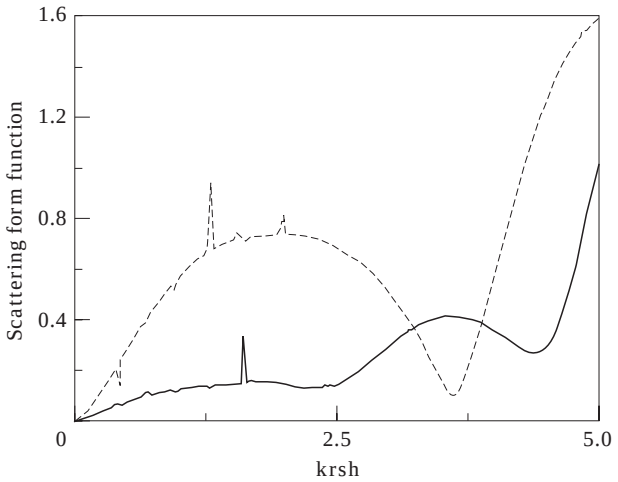

Figure 11. Effect of outer radius of an unlined steel cylinder on the scattering form function. ——, $r_{out} = 100$ mm; – – –, $r_{out} = 250$ mm.

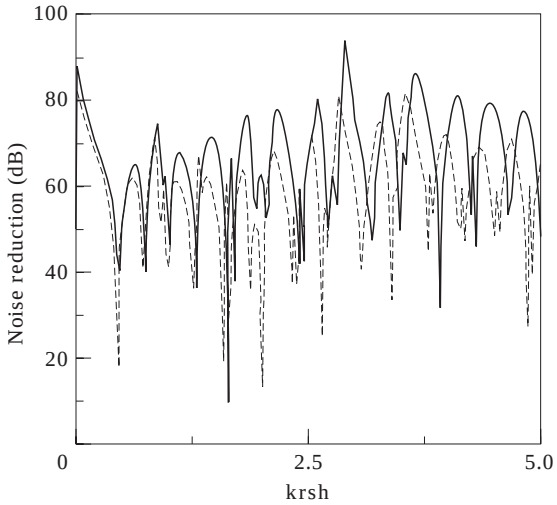

Figure 12. Effect of outer radius of an unlined steel cylinder on its noise reduction. ——, $r_{out} = 100$ mm; – – –, $r_{out} = 250$ mm.

There are hoses like those used in automotive climate control systems where the hose wall is made up of four layers of different types of elastomers or polymers. The transfer matrix method can tackle this four-layer cylindrical hose with equal ease. Results are shown are Figures 15 and 16 for the two configurations shown in Table 3. Each of the four layers in either configuration is 5 mm thick. The outermost radius is 100 mm as for the previous cases. The medium is air on the outside as well as inside.

It may be observed from Figure 15 that reversing the order of the layers has little effect on the scattering form function, where the two curves are completely overlapping. This is typical of the symmetrical nature of impedance mismatch, as shown for sudden expansion and contraction in reference [18] and for change in media in reference [20]. However, the curvature effect of the cylindrical surfaces produces considerable differences

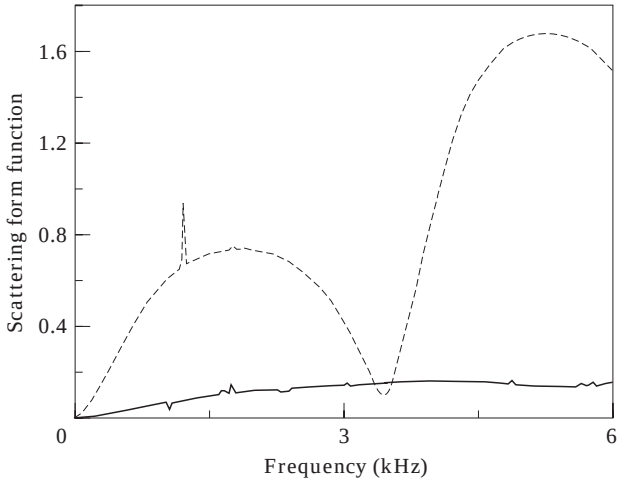

Figure 13. Effect of outer radius of an unlined steel cylinder on the scattering form function. ——, $r_{out} = 100$ mm; – – –, $r_{out} = 250$ mm.

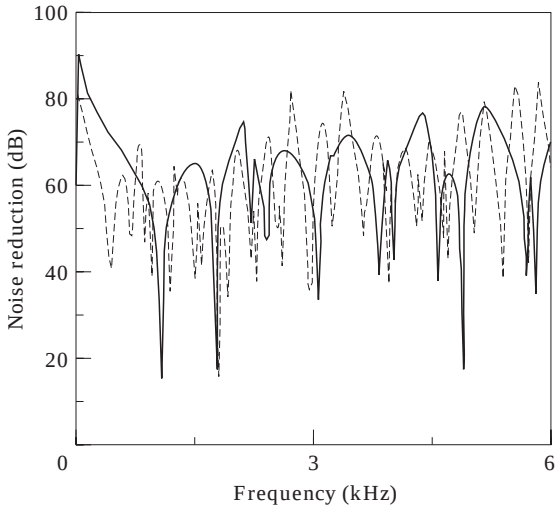

Figure 14. Effect of outer radius of an unlined steel cylinder on its noise reduction. ——, $r_{out} = 100$ mm; – – –, $r_{out} = 250$ mm.

in the noise reduction values as may be noted from Figure 16. This effect has also been observed in the interchange of the rubber and steel layers, although it is not shown here. Nevertheless, the primary purpose of Figures 15 and 16 is to show that the transfer matrix method may be applied readily to any number of layers, where the classical approach would be too cumbersome and susceptible to numerical instabilities.

7. CONCLUDING REMARKS

The transfer matrix presented here can be easily adapted to small or personal computers to evaluate the response of a multi-layer cylinder excited by a plane wave with one-dimensional pressure excitation. The overall transfer matrix elements can be obtained by multiplying the transfer matrices of successive layers by feeding in the elastic properties for the respective layers. Expressions are given for the evaluation of acoustic characteristics

TABLE 3

Hose configurations

	Poisson's ratio μ	Density ρ (kg/m^3)	Storage modulus E_r (Pa)	Loss factor η
Configuration (a)				
Layer 1	0·49	1200	$3{\cdot}3 \times 10^7$	0·8
Layer 2	0·47	1250	$3{\cdot}3 \times 10^8$	0·6
Layer 3	0·45	1300	$3{\cdot}3 \times 10^9$	0·4
Layer 4	0·43	1350	$3{\cdot}3 \times 10^{10}$	0·2
Configuration (b)				
Layer 1	0·43	1350	$3{\cdot}3 \times 10^{10}$	0·2
Layer 2	0·45	1300	$3{\cdot}3 \times 10^9$	0·4
Layer 3	0·47	1250	$3{\cdot}3 \times 10^8$	0·6
Layer 4	0·49	1200	$3{\cdot}3 \times 10^7$	0·8

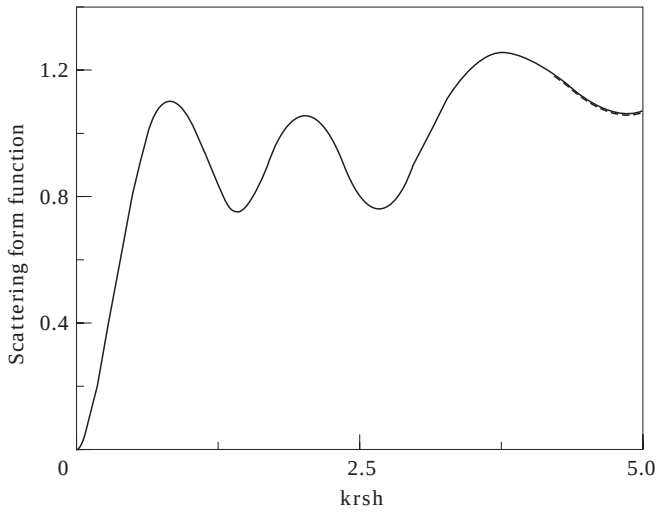

Figure 15. Scattering form function of a four-layer hose. ——, Configuration (a); – – –, configuration (b).

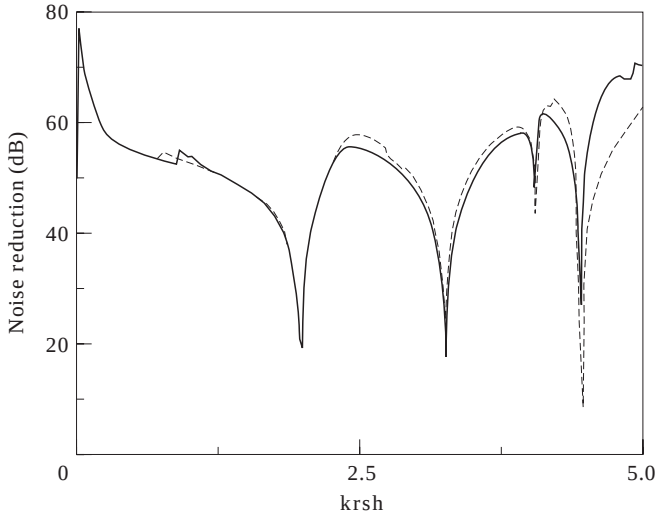

Figure 16. Noise reduction of a four-layer hose. ——, Configuration (a); – – –, configuration (b).

of the multi-layer cylinder. Numerical examples have been presented to illustrate the effect of type of layer, type of closure and variation of thickness of either of the two constituent layers on scattering form function and noise reduction of a two-layer cylinder.

ACKNOWLEDGMENTS

The authors would like to thank Dr S. V. Raman, of NSTL and Mr. P. S. Kasthurirangan of GTRE, for the help and encouragement given to one of the authors [JSS] during the course of this work.

REFERENCES

1. J. J. Faran 1951 *Journal of the Acoustical Society of America* **23**, 405–418. Sound scattering by solid cylinders and spheres.
2. M. C. Junger 1952 *Journal of the Acoustical Society of America* **24**, 366–373. Sound scattering by thin elastic shells.
3. R. D. Doolittle and H. Überall 1966 *Journal of the Acoustical Society of America* **39**, 272–275. Sound scattering by elastic cylindrical shells.
4. L. Flax and W. G. Neubauer 1977 *Journal of the Acoustical Society of America* **61**, 307–312. Acoustic reflection from layered elastic absorptive cylinders.
5. G. C. Gaunaurd 1977 *Journal of the Acoustical Society of America* **61**, 360–368. Sonar cross-section of a coated hollow cylinder in water.
6. L. Flax, L. R. Dragonette and H. Überall 1978 *Journal of the Acoustical Society of America* **63**, 723–731. Theory of elastic resonance excitation by sound scattering.
7. G. C. Gaunaurd and D. Brill 1984 *Journal of the Acoustical Society of America* **75**, 1680–1693. Acoustic spectrogram and complex-frequency poles of a resonantly excited elastic tube.
8. J. W. Dickey, D. A. Nixon and J. M. D'Archangelo 1983 *Journal of the Acoustical Society of America* **74**, 294–304. Acoustic high-frequency scattering by elastic cylindrical shells.
9. T. A. K. Pillai, V. K. Varadan, V. V. Varadan and R. P. Radinski 1983 *Journal of the Acoustical Society of America* **74**, 619–624. Acoustic wave scattering by elastic cylindrical shells in water.
10. M. F. Werby and L. H. Green 1983 *Journal of the Acoustical Society of America* **74**, 625–630. An extended unitary approach for acoustical scattering from elastic shells immersed in a fluid.
11. A. Akay 1991 *Journal of the Acoustical Society of America* **89**, Part 1, 1572–1578. Scattering of sound from concentric cylindrical shells.
12. F. Leon, F. Lecroq, D. Decultot and G. Maze 1992 *Journal of the Acoustical Society of America* **91**, 1388–1397. Scattering of an obliquely incident acoustic wave by an infinite hollow cylindrical shell.
13. X.-L. Bao, H. Cao and H. Überall 1990 *Journal of the Acoustical Society of America* **87**, 106–110. Resonances and surface waves in the scattering of an obliquely incident acoustic field by an infinite elastic cylinder.
14. W. T. Thomson 1950 *Journal of Applied Physics* **21**, 89–93. Transmission of elastic waves through a stratified solid medium.
15. N. A. Haskell 1953 *Bulletin of the Seismological Society of America* **43**, 17–34. The dispersion of surface waves in multi-layered media.
16. A. H. Nayfeh 1991 *Journal of the Acoustical Society of America* **89**, Part 1, 1521–1531. The general problem of elastic wave propagation in multi-layered anisotropic media.
17. M. L. Munjal 1992 *Journal of Sound and Vibration* **162**, 333–344. Response of a multi-layered infinite plate to an oblique plane wave by means of transfer matrices.
18. M. L. Munjal 1987 *Acoustics of Ducts and Mufflers*. New York: Wiley Interscience.
19. J. S. Sastry and M. L. Munjal 1995 *Journal of Sound and Vibration* **182**, 109–128. A transfer matrix approach for evaluation of the response of a multi-layered infinite plate to a two-dimensional pressure excitation.
20. L. Cremer and M. Heckl 1988 *Structure Borne Sound*. Berlin: Springer Verlag; second edition.
21. M. Abramowitz and I. A. Stegun 1964 *Handbook of Mathematical Functions*. Washington D.C.: National Bureau of Standards; first edition.

APPENDIX A

The elements of the transfer matrix of equation (46) are as follows:

$$A_{11} = \frac{\pi}{2}\left\{-k_L\,\lambda r_{in}\,R_{n,L} - \frac{2r_{in}}{r_{out}}\,S_{n,L} + \frac{k_T\,F}{r_{out}}\,Q_{n,T} - \frac{F}{r_{out}^2}\,P_{n,T}\right\},$$

$$A_{12} = \frac{\pi}{2}\left\{\lambda n P_{n,L} + \frac{k_L\,F}{n r_{out}}\,Q_{n,L} - \frac{k_T^2 F r_{in}}{n r_{out}}\,S_{n,T} + \frac{k_T\,F r_{in}}{n r_{out}^2}\,R_{n,T}\right\},$$

$$A_{13} = -\frac{\pi}{2}\frac{2G}{\mathrm{j}\omega}\left\{-k_L\, n\lambda R_{n,L} - \frac{k_L^2 F}{nr_{out}}\, S_{n,L} + \lambda\,\frac{n}{r_{in}}\, P_{n,L} + \frac{k_L\, F}{nr_{in}\, r_{out}}\, Q_{n,L} - \frac{k_T^2 F}{nr_{out}}\, S_{n,T}\right.$$

$$\left. - \xi\,\frac{k_T\, nr_{in}}{r_{out}}\, Q_{n,T} + \xi\,\frac{nr_{in}}{r_{out}^2}\, P_{n,T} + \frac{k_T\, F}{nr_{out}^2}\, R_{n,T}\right\},$$

$$A_{14} = -\frac{\pi}{2}\frac{2G}{\mathrm{j}\omega}\left\{-k_L\,\lambda R_{n,L} - \frac{k_L^2 F}{n^2 r_{out}}\, S_{n,L} - \frac{k_T^2 r_{in}}{2}\,\xi\lambda P_{n,L}\right.$$

$$\left. - \frac{k_L\, r_{in}}{r_{out}}\,\xi Q_{n,L} - \frac{k_T^2 F}{r_{out}}\, S_{n,T} + \frac{k_T\, F}{r_{in}\, r_{out}}\, Q_{n,T} - \frac{F}{r_{in}\, r_{out}^2}\, P_{n,T} + \frac{k_T\, F}{r_{out}^2}\, R_{n,T}\right\},$$

$$A_{21} = \frac{\pi}{2}\left\{\lambda n P_{n,T} + \frac{k_L\, F r_{in}}{nr_{out}^2}\, R_{n,L} - \frac{k_L^2 F r_{in}}{nr_{out}}\, S_{n,L} + \frac{k_T\, F}{nr_{out}}\, Q_{n,T}\right\},$$

$$A_{22} = \frac{\pi}{2}\left\{-k_T\,\lambda r_{in}\, R_{n,T} - \frac{2r_{in}}{r_{out}}\, S_{n,T} + \frac{k_L\, F}{r_{out}}\, Q_{n,L} - \frac{F}{r_{out}^2}\, P_{n,L}\right\},$$

$$A_{23} = -\frac{\pi}{2}\frac{2G}{\mathrm{j}\omega}\left\{-\xi\lambda\,\frac{k_T^2 r_{in}}{2}\, P_{n,T} - k_T\,\lambda R_{n,T} + \frac{k_L\, F}{r_{out}^2}\, R_{n,L}\right.$$

$$\left. - \xi\,\frac{k_T\, r_{in}}{r_{out}}\, Q_{n,T} - \frac{F}{r_{in}\, r_{out}^2}\, P_{n,L} - \frac{k_L^2 F}{r_{out}}\, S_{n,L} + \frac{k_L\, F}{r_{in}\, r_{out}}\, Q_{n,L} - \frac{k_T^2 F}{n^2 r_{out}}\, S_{n,T}\right\},$$

$$A_{24} = -\frac{\pi}{2}\frac{2G}{\mathrm{j}\omega}\left\{\frac{k_L\, F}{nr_{out}^2}\, R_{n,L} + \xi\,\frac{nr_{in}}{r_{out}^2}\, P_{n,L} - \frac{k_L^2 F}{nr_{out}}\, S_{n,L} - \frac{k_L\, nr_{in}}{r_{out}}\,\xi Q_{n,L}\right.$$

$$\left. - \frac{k_T^2 F}{nr_{out}}\, S_{n,T} + \frac{k_T\, F}{nr_{in}\, r_{out}}\, Q_{n,T} - k_T\, n\lambda R_{n,T} + \frac{n}{r_{in}}\,\lambda P_{n,T}\right\},$$

$$A_{31} = \frac{\pi}{2}\frac{\mathrm{j}\omega n}{Gk_T^2}\left\{k_T\, Q_{n,T} + \frac{r_{in}}{r_{out}}\, k_L\, R_{n,L}\right\}, \qquad A_{32} = -\frac{\pi}{2}\frac{\mathrm{j}\omega}{Gk_T^2}\left\{k_T^2 r_{in}\, S_{n,T} + \frac{n^2}{r_{out}}\, P_{n,L}\right\},$$

$$A_{33} = \frac{\pi}{2}\left\{-\frac{k_L\, F}{r_{out}}\, R_{n,L} + 2S_{n,T} + \frac{F}{r_{in}\, r_{out}}\, P_{n,L} + \xi k_T\, r_{in}\, Q_{n,T}\right\},$$

$$A_{34} = \frac{\pi}{2}\left\{-\frac{k_L\, F}{nr_{out}}\, R_{n,L} + \frac{k_T^2 F}{n}\, S_{n,T} - \frac{k_T\, F}{nr_{in}}\, Q_{n,T} - \xi\,\frac{nr_{in}}{r_{out}}\, P_{n,L}\right\},$$

$$A_{41} = -\frac{\pi}{2}\frac{\mathrm{j}\omega}{Gk_T^2}\left\{k_L^2 r_{in}\, S_{n,L} + \frac{n^2}{r_{out}}\, P_{n,T}\right\}, \qquad A_{42} = \frac{\pi}{2}\frac{\mathrm{j}\omega n}{Gk_T^2}\left\{k_L\, Q_{n,L} + \frac{r_{in}}{r_{out}}\, k_T\, R_{n,T}\right\},$$

$$A_{43} = \frac{\pi}{2}\left\{ -\frac{k_L F}{nr_{in}} Q_{n,L} + \frac{k_L^2 F}{n} S_{n,L} - \frac{k_T F}{nr_{out}} R_{n,T} - \xi \frac{nr_{in}}{r_{out}} P_{n,T} \right\},$$

$$A_{44} = \frac{\pi}{2}\left\{ \frac{2k_L^2}{k_T^2} S_{n,L} + \xi k_L r_{in} Q_{n,L} - \frac{k_T F}{r_{out}} R_{n,T} + \frac{F}{r_{in} r_{out}} P_{n,T} \right\}.$$

Here

$$\begin{aligned}
P_{n,L} &= \mathrm{J}_n(k_L r_{in})\mathrm{Y}_n(k_L r_{out}) - \mathrm{Y}_n(k_L r_{in})\mathrm{J}_n(k_L r_{out}),\\
Q_{n,L} &= \mathrm{J}_n(k_L r_{in})\mathrm{Y}'_n(k_L r_{out}) - \mathrm{Y}_n(k_L r_{in})\mathrm{J}'_n(k_L r_{out}),\\
R_{n,L} &= \mathrm{J}'_n(k_L r_{in})\mathrm{Y}_n(k_L r_{out}) - \mathrm{Y}'_n(k_L r_{in})\mathrm{J}_n(k_L r_{out}),\\
S_{n,L} &= \mathrm{J}'_n(k_L r_{in})\mathrm{Y}'_n(k_L r_{out}) - \mathrm{Y}'_n(k_L r_{in})\mathrm{J}'_n(k_L r_{out}),\\
P_{n,T} &= \mathrm{J}_n(k_T r_{in})\mathrm{Y}_n(k_T r_{out}) - \mathrm{Y}_n(k_T r_{in})\mathrm{J}_n(k_T r_{out}),\\
Q_{n,T} &= \mathrm{J}_n(k_T r_{in})\mathrm{Y}'_n(k_T r_{out}) - \mathrm{Y}_n(k_T r_{in})\mathrm{J}'_n(k_T r_{out}),\\
R_{n,T} &= \mathrm{J}'_n(k_T r_{in})\mathrm{Y}_n(k_T r_{out}) - \mathrm{Y}'_n(k_T r_{in})\mathrm{J}_n(k_T r_{out}),\\
S_{n,T} &= \mathrm{J}'_n(k_T r_{in})\mathrm{Y}'_n(k_T r_{out}) - \mathrm{Y}'_n(k_T r_{in})\mathrm{J}'_n(k_T r_{out}),\\
\xi &= (1 - F/r_{in}^2), \qquad \lambda = (1 - F/r_{out}^2), \qquad F = 2n^2/k_T^2.
\end{aligned}$$

APPENDIX B

The elements of A_{ij} required to calculate the scattering coefficient b_n of equation (88) for the case of a solid cylinder are as follows:

$$A_{13} = -\frac{2G}{\mathrm{j}\omega}\left\{ k_L \lambda n \mathrm{J}_n(k_L r_{out}) + \frac{k_L^2 F}{nr_{out}} \mathrm{J}'_n(k_L r_{out}) + \frac{k_T^2 F}{nr_{out}} \mathrm{J}'_n(k_T r_{out}) - \frac{k_T F}{nr_{out}^2} \mathrm{J}_n(k_T r_{out}) \right\},$$

$$A_{14} = -\frac{2G}{\mathrm{j}\omega}\left\{ k_L \lambda \mathrm{J}_n(k_L r_{out}) + \frac{k_L^2 F}{n^2 r_{out}} \mathrm{J}'_n(k_L r_{out}) + \frac{k_T^2 F}{r_{out}} \mathrm{J}'_n(k_T r_{out}) - \frac{k_T F}{r_{out}^2} \mathrm{J}_n(k_T r_{out}) \right\},$$

$$A_{23} = -\frac{2G}{\mathrm{j}\omega}\left\{ k_T \lambda \mathrm{J}_n(k_T r_{out}) - \frac{k_L F}{r_{out}^2} \mathrm{J}_n(k_L r_{out}) + \frac{k_L^2 F}{r_{out}} \mathrm{J}'_n(k_L r_{out}) + \frac{k_T^2 F}{n^2 r_{out}} \mathrm{J}'_n(k_T r_{out}) \right\},$$

$$A_{24} = -\frac{\pi}{2}\frac{2G}{\mathrm{j}\omega}\left\{ -\frac{k_L F}{nr_{out}^2} \mathrm{J}_n(k_L r_{out}) + \frac{k_L^2 F}{nr_{out}} \mathrm{J}'_n(k_L r_{out}) + \frac{k_T^2 F}{nr_{out}} \mathrm{J}'_n(k_T r_{out}) + k_T n \lambda \mathrm{J}_n(k_T r_{out}) \right\},$$

$$A_{43} = \left\{ -\frac{k_L^2 F}{n} \mathrm{J}'_n(k_L r_{out}) + \frac{k_T F}{nr_{out}} \mathrm{J}_n(k_T r_{out}) \right\},$$

$$A_{44} = \left\{ -\frac{2k_L^2}{k_T^2} \mathrm{J}'_n(k_L r_{out}) + \frac{k_T F}{r_{out}} \mathrm{J}_n(k_T r_{out}) \right\}.$$

Here

$$\lambda = (1 - F/r_{out}^2), \qquad F = 2n^2/k_T^2.$$